

Investigation of equilibrium and stability of self-contracted discharges in an optically dense plasma

A. F. Aleksandrov, V. V. Zosimov, A. A. Rukhadze, V. I. Savoskin, and I. B. Timofeev

Moscow State University

(Submitted December 18, 1972)

Zh. Eksp. Teor. Fiz. **64**, 1568-1580 (May 1973)

The region of existence and the main parameters of a strong-current self-contracted opaque discharge produced by electric explosion of wires of various metals are investigated. It is found experimentally that an opaque equilibrium discharge with a homogeneous temperature exists in a rather narrow range of discharge currents from ~ 100 – 130 to ~ 300 kA. The absolute value of the brightness temperature grows with increase of the discharge current and decrease of the number of particles in the discharge. The characteristic sizes and electric characteristics of the discharge and also the radiation outputs in various spectral intervals and the energy balance are determined. It is shown that discharges with lengths considerably exceeding their diameter are subject to instabilities of the neck and kink types. Their development increments, which depend on the velocity of isothermal sound, are also determined. The experimental results are compared with the theoretical calculations and satisfactory agreement is found. As radiation sources, the discharges studied possess about the same characteristics as selective discharges in lithium or atmospheric discharges.

1. INTRODUCTION

Strong-current self-contracted discharges (pinches) have been investigated intensively of late from the point of view of their use as radiation sources for laser pumping^[1-16]. The theory of such discharges has been developed in sufficient detail, and, in particular, the equilibrium characteristics of strong-current discharges have been investigated in transparent^[1-5], opaque^[1-3,6], and grey^[7] plasmas for both direct and alternating^[8] current, and computer calculation methods have been developed for the nonstationary processes in such discharges^[9]. However, one can regard only linear pinches in an optically transparent plasma as adequately investigated experimentally. This concerns primarily transparent discharges in a lithium plasma, the investigation of which has been the main subject of a cycle of studies performed at the Physics Institute of the USSR Academy of Sciences (FIAN)^[10-13,15,16]. In these investigations, careful studies were made of the absorption coefficients, of the total yield and of the spectral composition of the radiation^[10-14], of the spatial distribution of the parameters^[13-15], of the energy balance in the discharge^[11], and of the discharge stability^[16]. These investigations, on the one hand, confirmed rather well the correctness of the theoretical concepts developed for transparent lithium discharges and, on the other hand, point to their good qualities as radiation sources, namely greater brightness and good selectivity. The same investigations, however, while not directly confirming the proneness of discharges in a transparent plasma to develop superheat instability rapidly, nonetheless offer evidence of their complex irregular structure, which undoubtedly is a shortcoming in a radiation source.

At the same time, no systematic investigations have been made of opaque pinches in an atmosphere of heavy gases, which should have a much greater stability than the aforementioned lithium discharges. There are quite a number of published papers in which such discharges

were produced by electric explosion of wires in vacuum^[17-21]. Most of these papers are devoted to the dynamics of such discharges, and only a few cite data on the characteristics of the opaque stage of the discharge. Thus, the presence of a pinch effect accompanied by the appearance of a continuous spectrum and an increasing discharge temperature has been demonstrated^[17-20], as well as the development of magnetohydrodynamic instabilities in such discharges. Only two investigations^[15,20] have demonstrated convincingly that a discharge plasma in indium or aluminum vapor contains regions with uniform temperature distribution, emitting black-body radiation in the spectral transmission band of quartz. However, the data cited in these papers are utterly insufficient both from the point of view of verifying the theory of the strong-current pinch in an optically dense plasma and from the point of view of investigating the characteristics of such discharges as radiation sources. The researches reported below fill this gap to some degree.

2. FUNDAMENTAL THEORETICAL RELATIONS

To facilitate the subsequent exposition, we present first the principal results of the theory of strong-current self-contracted discharges in an optically dense plasma in a form that is convenient for practical applications^[1,3,22]. As shown by the analysis, all the principal parameters of the discharge can be expressed in terms of the discharge current I and the total number of particles per unit discharge length N_t . In particular, for the plasma temperature $T_0(t)$ on the discharge axis and for the characteristic discharge dimensions $r_d(t)$ we have

$$T_0(t) = 3.6 \cdot 10^{13} \frac{I^2(t)}{(1+z)N_t} \text{ [}^\circ\text{K]}, \quad (2.1)$$

$$r_d(t) = 8.15 \cdot 10^{-21} z^{1/2} (1+z)^{1/4} \frac{N_t}{I^2(t)} \text{ [cm]}, \quad (2.2)$$

where z is the average ion charge, I is expressed in

amperes, and N_{\dagger} is given in cm^{-3} . In the derivation of these formulas we assumed that the temperature and the electric field are homogeneous over the discharge cross section (the density distribution over the cross section is parabolic), that the discharge is optically opaque, and that it is formed in a quasistationary manner.

The applicability of the radiant thermal conductivity approximation and the requirement that the temperature be uniform impose a limitation on the discharge current:

$$I_{\text{cr min}} < I < I_{\text{cr max}}, \quad (2.3)$$

where the values of the critical current (the minimal $I_{\text{cr min}}$ and the maximal $I_{\text{cr max}}$) depend on the mechanism whereby light is radiated in the discharge. In the case of multiple ionization, they are universal constants and equal to $I_{\text{cr min}} \approx 130$ kA and $I_{\text{cr max}} \approx 420$ kA, independently of the type of material in the discharge. At $I < I_{\text{cr min}}$, the Rosseland free path of the quanta in the discharge becomes larger than r_d , and at $I \approx I_{\text{cr max}}$ the distribution of the temperature in the discharge should become inhomogeneous to the same degree as the inhomogeneity of the density.

The requirement that the electric field be homogeneous leads to the following lower bound on the total number of particles N_{\dagger} :

$$N_{\dagger}^{1/2} \gg 6 \cdot 10^{-2} \frac{(1+z)^{1/2}}{z^{3/2}} \frac{I}{A^{1/2}}, \quad (2.4)$$

where A is the atomic weight of the ions in the discharge.

With the aid of formulas (2.1) and (2.2) we can also obtain expressions for other parameters that characterize the discharge, such as the plasma density, the electric field intensity, and the active resistance of the discharge. As to the radiation from the surface of the discharge, it coincides in the considered approximation with absolute black-body radiation. Realistically, however, the radiation from the discharge never coincides with black body radiation, owing to the transparency to the short-wave quanta. In such semitransparent (grey) discharges it is possible however to have, a state with a homogeneous temperature, owing to the large radiant thermal conductivity for the long-wave quanta. The radiation of such grey discharges is described approximately by the relation

$$S = \hat{\sigma} T^4 \xi(x_0), \quad (2.5)$$

$$\xi(x_0) = \frac{15}{\pi^4} \int_0^{\infty} \frac{x^3 dx}{e^x - 1} + \frac{10}{\pi^4} \frac{x_0^3}{\exp x_0 - 1},$$

σ is the Stefan-Boltzmann constant, $x_0 = h\nu_0/kT$ is a dimensionless quantum frequency corresponding to equality of the spectral mean free path $l(\nu_0)$ to the characteristic discharge dimension r_d , i.e., to equality of the optical thickness of the discharge to unity:

$$\tau(\nu_0) = \kappa_{\nu}(\nu_0) r_d(\nu_0) = r_d(\nu_0) / l(\nu_0) = 1. \quad (2.6)$$

When $\nu > \nu_0$, the plasma is assumed to be fully transparent, and at $\nu < \nu_0$ completely opaque.

The temperature in a grey discharge is given by formula (2.1), and the radius r_d is decreased by a factor $\xi^{1/3}(x_0)$. The value of x_0 itself is calculated at a given I from Eq. (2.6) by a graphic method. The region of existence of a grey discharge with homogeneous temperature is broader than the region of existence of an opaque discharge, owing to the decrease of the minimal critical current by a factor of 2 - 3.

Finally, it should be noted that the discharges in question have equal stability, since no superheat large-

scale instability can develop in them, and the growth increments of the most dangerous fundamental surface mode of the necking instability is equal to

$$\gamma = (12\alpha^2)^{1/2} \nu_e / r_d, \quad (2.7)$$

where $\alpha^2 = k_z^2 r_d^2$ is a small parameter of the theory, i.e., $\alpha^2 \ll 1$. The growth increment of the rather dangerous long-wave flexural instability modes is also smaller by a factor $\alpha^{-1/2}$.

3. EXPERIMENTAL PROCEDURE

To produce a self-contracted discharge in an optically dense plasma with constant total number of particles we used, as in the papers described in Sec. 1, electrical explosion of wires in vacuum.

The experiments were performed with two discharge circuits with capacitive energy storage, having different energy capacities and different periods. The first installation, which was described earlier^[22-24], stored up to 30 kJ and had a capacitance of either 54 or 72 μF , and the period, depending on the length of the exploded wire, fluctuated somewhat about 25 μsec . The second discharge circuit could store up to ~ 250 kJ and had a much longer period, the first half-cycle of the discharge current reaching 80 μsec in the experiments. This installation was also described in detail earlier^[25]. The two installations could be charged to a working voltage $U_0 = 30$ kV.

The discharge chamber consisted of two flat steel electrodes, between which the exploded wire, ranging in length from 5 to 100 cm, was stretched. The electrodes were placed in a quartz tube which was clamped vacuum-tight between the upper electrode and the metallic disk that served as the ground of the circuit, with the aid of 8 cylindrical copper tightening bolts that served as the return current lead. With such a construction, the chamber in the working state constituted the equivalent of a coaxial cable. The discharge chamber was evacuated to a pressure no higher than 10^{-5} mm Hg. We used wires of aluminum, copper, silver, and tungsten.

The diagnostics methods used in the study were analogous to those already used and described in detail in^[11,22-25], and we shall therefore only list them briefly. The shape and the characteristic dimensions of the discharge were investigated with the aid of an SFR-2M camera, and the current-voltage characteristics were plotted with the aid of Rogowski loops and noninductive voltage dividers. The time-swept emission spectrum of the discharge was registered by using disk slit scanning and an ISP-30 spectrograph. The discharge radiation in individual spectral intervals was registered with F-1 and F-7 photocells and light filters. A standard source of type EV-45 was used for the absolute calibration. The integrated radiation energy in the transparency region of quartz was measured with the aid of a calorimeter.

The first setup was used to investigate the principal characteristics of the equilibrium stage of the discharge^[22,23,26] and its stability^[22,24], while the second was used to obtain data on the investigated discharge as a source of radiation^[1,26].

4. INVESTIGATION OF THE STAGE OF MAGNETIC CONFINEMENT

In this section we present the results of an investigation of the region of existence and the principal para-

meters of an opaque discharge maintained in equilibrium by the magnetic field of the discharge current itself. The experiments were performed with the first setup, and the capacitance of the discharge circuit was $54 \mu\text{F}$.

The equilibrium characteristics were investigated for relatively short discharge gaps, 5 cm long. In this case, the discharge was nearly periodic (see Fig. 1a), with a period $\sim 25 \mu\text{sec}$ and a damping decrement $\sim 0.25 - 0.3$. At discharge voltages $U_0 = 15, 20,$ and 30 kV , the amplitudes of the current in the first maximum were 160, 220, and 380 kA. Thus, the experiment covered the entire discharge-current range defined by the inequalities (2.3).

We exploded wires with diameters from 9×10^{-2} to 0.5 mm; the number of particles per unit length of wire ranged from $4.6 \times 10^{18} \text{ cm}^{-1}$ to $\sim 1.2 \times 10^{20} \text{ cm}^{-1}$.

The high-speed photographs of the "short" discharges revealed a discharge of strictly cylindrical shape without any deviations. Only during the later stages of the discharge ($70 - 80 \mu\text{sec}$) did there appear small-scale perturbations of the discharge surface. This high stability of the discharge surface is apparently due to the stabilizing influence of the electrodes. The photographs were used to determine the dependence of the radius of the plasma filament on the time. A typical time dependence of the discharge channel obtained in this manner is shown in Fig. 2 for the case of explosion of a silver wire of 0.09 mm diameter at $U_0 = 15 \text{ kV}$. A similar picture was also observed under other experimental conditions (different wire diameters and materials, different working voltages). From experimental plots similar to that shown here it can be established that at different instants of time the radius of the channel increases at a rate $(3 - 6) \times 10^6 \text{ cm/sec}$, depending on the initial voltage and on the number of particles per unit discharge length. This stage was followed, in all the investigated cases, by a stage of magnetic confinement near the first maximum of the current (Fig. 2). Figure 3 shows the dependence of the discharge-channel radius on the discharge current for exploding "thin" silver wires (diameter 0.1 mm, $N_t = 5 \times 10^{18} \text{ cm}^{-1}$). The experimental points correspond to the start of the stage of magnetic confinement (the time instant $t = 2.5 \mu\text{sec}$ from the start of the discharge) at different voltages (15 - 30 kV). It is seen from the figure that the radius of the discharge channel decreases monotonically with increasing discharge current.

We now examine the spectral characteristics of the discharge. A typical time sweep of the spectrum is shown in Fig. 1b. We see that the first to appear is a continuous spectrum, with the main fraction of the radiation energy released during the first half-cycle in the form of continuous radiation. Then, after time intervals equal to half the discharge-current cycle, several weaker maxima of radiation intensity are observed, and in these regions the radiation also seems to be almost entirely continuous. In the gaps between the maxima of the continuous radiation, the spectrum has a complicated character, with a complicated line spectrum superimposed on the continuous spectrum. The continuous spectrum was used to determine the brightness temperature of the discharge, which corresponds to the true temperature of the discharge surface in the region where the radiation is of the black-body type, as verified carefully for different instants of time during the first half-cycle of the current. It was assumed that the discharge radiates as an absolutely black body if the brightness temperature T does not depend, within the limits of measurement

errors, on the wavelength λ in the entire registered spectral interval. A similar check, which will be discussed in detail later on, has shown that the radiation has a black-body character in the entire region of magnetic confinement.

The circles in Fig. 4 represent the time dependence of the brightness temperature, obtained by this method, for the case of explosion of a "thin" wire (0.1 mm diameter) at 15 and 30 kV. It is seen from the figure that the time variation of the brightness temperature in the first half-cycle follows the variation of the discharge

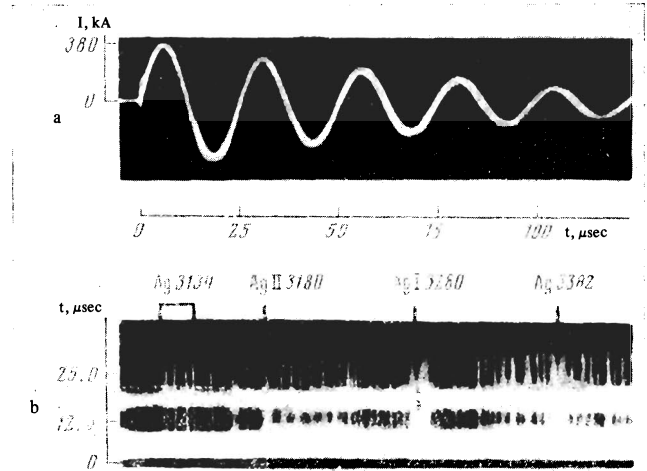


FIG. 1. Current oscillogram obtained following explosion of a silver wire of 0.09 mm diameter at a capacitor-bank voltage $U_0 = 30 \text{ kV}$ (a) and section of the time sweep of the spectrum under the same conditions (b).

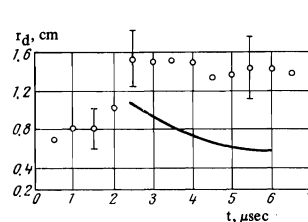


FIG. 2

FIG. 2. Time dependence of the radius r_d of the discharge channel. Silver wire, 0.09 mm diameter, $U_0 = 15 \text{ kV}$. The experimental values are represented by points and the solid curve was obtained by theoretical calculation.

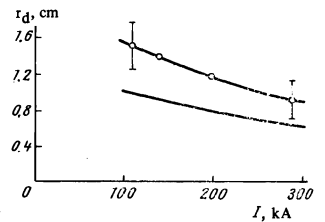


FIG. 3

FIG. 3. Dependence of r_d on the discharge current I . Silver wire, 0.1 mm diameter, $U_0 = 15 \text{ kV}$.

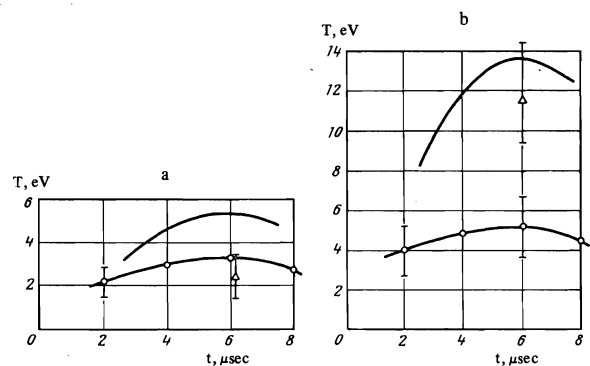


FIG. 4. Time dependence of the discharge temperature T . Silver wire, 0.09 mm diameter. \circ - brightness temperature, Δ - calculated from the conductivity, solid curve - theoretical calculation. a - $U_0 = 15 \text{ kV}$, b - $U_0 = 30 \text{ kV}$.

current. At the maxima of the current, the temperature values reached in this case are 3 – 5 eV, depending on the applied voltage and on the wire diameter. A similar temperature variation follows from the data obtained with the photocells. From the oscillograms of the signals obtained from the F-1 photocells (which registered the spectral interval from 3350 to 4350 Å) and the F-7 photocells (2300 – 3300 Å) it follows also that the principal fraction of the energy is radiated in the first half-cycle of the current, in agreement with the conclusion drawn from the analysis of the spectrograms.

Using the standard procedure^[25], we also calculated the temperature averaged over the cross section of the discharge filament, by starting from the current-voltage characteristics of the discharge at the instant of the first current maximum. We used for this purpose the expression for the conductivity of a fully-ionized plasma, and the function $z(T)$ was determined in accordance with the usual Kramers-Unsold procedure. The values of T obtained in this manner are shown by triangles in Fig. 4. We see that at $U_0 = 15$ kV the brightness temperature and the temperature determined from the conductivity are practically the same.

Let us now dwell in greater detail on the dependence of the brightness temperature on the wavelength. Figure 5 shows the indicated dependence for discharges produced by explosion of silver^[23], aluminum, copper, and tungsten wires with different diameters at 15 kV. Curves 1, 2, and 3 pertain respectively to the 6-th, 4-th, and 2-nd microseconds from the start of the discharge, corresponding to discharge currents of 165, 130, and 70 kA. As can be seen from the figure, for discharges produced by explosion of wires of different materials and with different numbers of particles, the brightness temperature is independent of the wavelength, i.e., the discharge emits absolute black-body radiation (for example, the straight line 1), at instants of time exceeding a certain t_0 , i.e., for a discharge current exceeding a certain value. At current values lower than a certain $I_{cr.min}$, the discharge ceases to be a black emitter and the brightness temperature decreases with decreasing wavelength. The fact that the optical thickness is close to unity near $I_{cr.min}$ is also demonstrated by measurements made by passing through the discharge its own radiation reflected from a mirror, and also by passing light from an He-Ne laser through the discharge. We note that the plots presented were obtained by photometry of discharge spectra obtained at a constant initial voltage, but measured at different instants of time. Analogous plots can also be obtained by investigating the behavior of the discharge spectrum at the maximum of the current while the amplitude of the discharge current is varied (by varying the changing voltage).

The reduction of similar plots for the purpose of finding this minimum value $I_{cr.min}$ has shown that it lies in the range 100 – 130 kA and does not depend on the initial voltage U_0 , on the wire diameter, or on the wire material. Thus, $I_{cr.min}$ is a universal quantity that does not depend on N_t or on the wire material, and has an absolute value that agrees well with the theoretical value.

The fact that experiments reveal a clearly pronounced stage of magnetic confinement, and that in this region the discharge radiates like an absolute black body, enables us to use formulas (2.1) and (2.2) for its description. Here, as above, we used the theoretical $z(T)$ relation. The theoretical values of r_d and T obtained from these formulas, represented by the solid

curves of Figs. 2–4, agree well with the experimental data at small discharge currents. However, even the discrepancy observed at $U_0 = 30$ kV (see Fig. 4b) seems to have a profound physical nature. Indeed, the maximum discharge current reaches in this case 380 kA, which is close to the upper limiting current $I_{cr.max} = 420$ kA called for by the theory. On the other hand, the physical meaning of $I_{cr.max}$, as already mentioned in Sec. 2, is that at this value of the current the temperature in the discharge should become just as inhomogeneous over the discharge cross section as the density, i.e., it should decrease rapidly toward the surface of the discharge. Recalling furthermore that the brightness temperature corresponds to the temperature of the discharge surface, we can easily understand why the average value of T given by calculation or determined from measurements of quantities averaged over the discharge cross section (such as conductivity) greatly exceeds the true value of the surface temperature measured by the optical method.

In concluding this section, let us dwell also on the dependence of T on the total number of particles per unit length of the exploded wire, as shown in Fig. 6. The dashed curve in this figure shows the result of a theoretical calculation by means of formula (2.1), assuming that all the wire particles are captured in the discharge. It is seen that in the case of thick wires there is a strong discrepancy, which can be attributed to incomplete evaporation of the wire at those rates of energy supply to the discharge which obtained in the experiment. A tendency towards an increasing discrepancy between theory and experiment is also observed at small N_t . It may be due to violation of the inequality (2.4), since under our conditions we have $N_{cr} \approx 4 \times 10^{19}$ cm^{-1} at $I = 160$ kA.

5. STABILITY OF OPTICALLY OPAQUE DISCHARGE

The investigated short discharges, as follows from the results of the preceding section, were highly stable because their length was commensurate with the characteristic dimension of the discharge channel r_d , and because of the stabilizing influence of the electrodes. The stability of the equilibrium state of the discharge was therefore studied for relatively long ($l = 25$ cm) discharge gaps, for which $l \gg r_d$. The investigations

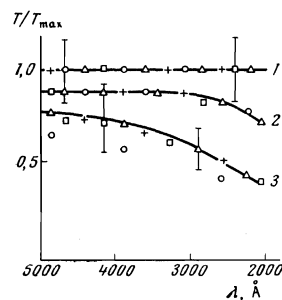


FIG. 5

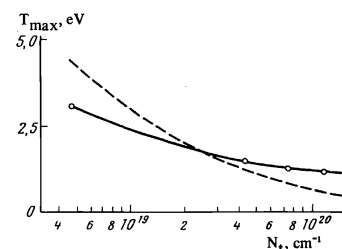


FIG. 6

FIG. 5. Dependence of the dimensionless brightness temperature on the wavelength. $U_0 = 15$ kV. The experimental points correspond to explosions: \square —Al, 0.3 mm diameter; \circ —Cu, 0.14 mm diameter; \triangle —Ag, 0.1 mm diameter; $+—$ W, 0.2 mm diameter. Curves 1, 2, and 3 pertain respectively to the sixth, fourth, and second microseconds from the start of the discharge.

FIG. 6. Dependence of the brightness temperature of the discharge on the total number of particles per unit length of a silver wire at $U_0 = 15$ kV.

were carried out with the first discharge circuit, with $72 \mu\text{F}$ capacitance. The discharge period however, remained, the same as before, $25 \mu\text{sec}$, as a result of a decrease in the parasitic inductance.

The radiation of these discharges has shown that near the first current maximum there is a clearly pronounced stage of magnetic confinement, but that the shape of the discharge is subject to clearly pronounced perturbations of the type of necking and kink instabilities. This is clearly seen from the photograph of an aluminum discharge (wire of 0.14 mm diameter) during the stage of magnetic confinement, as shown in Fig. 7, where the observed overall bending of the discharge filament is connected neither with any possible initial perturbation nor with the asymmetry of the turning on of the discharge chamber. At the same time we observed no data offering evidence of development of superheat instabilities.

For a quantitative investigation of the development of force instabilities, we separated the helical instabilities from the necking instabilities, and the functions characterizing the necking and helical perturbations were expanded in Fourier series. The analysis showed that an instability of the necking type has a maximum amplitude for the harmonics corresponding to $k_z r_d \approx (0.7 - 0.9) \leq 1$. For helical instabilities, the maximum amplitude is possessed by perturbations with $k_z r_d \approx 0.15$, corresponding to $k_z \approx \pi/l$, i.e., perturbations with a length equal to double the length of the discharge gap.

We have calculated the increments of instability development by comparing the amplitudes of the maximal harmonics for different instants of time. The increments γ obtained in this manner from high-speed photographs of explosions of aluminum, copper, silver, and tungsten wires are represented by the circles in Fig. 8 as functions of the atomic weight of the material of the exploded wires. The increments of the necking mode of instability are represented by curves 1, and those of the helical mode by curve 2. An investigation of the dependence of the stability increments on the speed of sound v_s , carried out both by measuring the discharge temperature and by measuring the mass of the ions in the discharge, has shown that the instability development increments are directly proportional to the speed of sound for both the necking and helical instabilities.

Figure 8 also shows, in the form of solid curves, the results of a theoretical calculation of the increments of

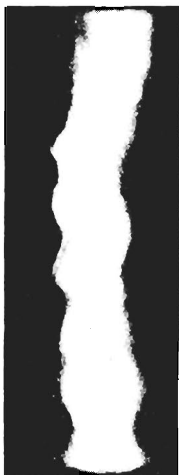


FIG. 7. Typical form of discharge with developed instability, photographed with SFR-2M camera at a rate of 1 frame per microsecond. The frame corresponding to the sixth microsecond of the discharge is shown. Explosion of aluminum wire of 0.14 mm diameter, $U_0 = 15 \text{ kV}$.

FIG. 8. Dependence of the increments of development of the fundamental mode of necking instability (curves 1) and helical instability (curves 2) on the atomic weight of the material of the exploded wire.

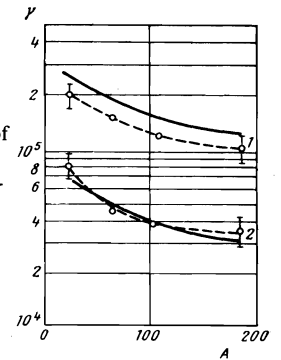
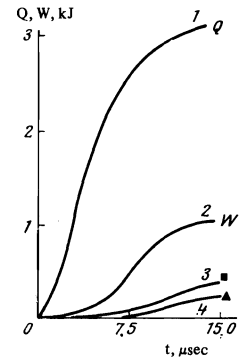


FIG. 9. Time dependence of the electric energy Q delivered to the discharge (curve 1) and the energy $W_{\Delta\lambda_1}$ radiated in the transparency band of quartz (curve 2). Curve 3 corresponds to the radiation in the band $\Delta\lambda_3 = 2300-3300\text{\AA}$, and curve 4 pertains to the band $\Delta\lambda_4 = 3300-4300\text{\AA}$. \blacktriangle —internal (thermal) energy U , \blacksquare —ionization energy I .



the development of the force instabilities in accordance with the relations given in Sec. 2 (see formula (2.7) ff.). Good quantitative agreement between theory and experiment is observed.

6. ENERGY BALANCE AND DISCHARGE RADIATION YIELD

We shall analyze the energy balance of the discharge using as an example the short discharges described in Sec. 3, and then present quantitative data concerning the principal energy characteristics, namely the electric energy Q released in the plasma and the radiation energy W . We express the equation of the energy balance in the discharge in the usual form:

$$Q = E_{ev} + E_{kin} + W_{\Delta\lambda_1} + W_{\Delta\lambda_2} + I + U. \quad (6.1)$$

Here Q is the energy delivered to the discharge, E_{ev} is the energy consumed in evaporation of the wire, E_{kin} is the kinetic energy of the expanding plasma column, $U = (1+z)NkT$ is the thermal energy of the plasma, I is the energy consumed in ionization, $W_{\Delta\lambda_1}$ is the energy radiated in the transparency band of quartz ($\Delta\lambda_1 = 2000 \text{ \AA} - \infty$), and $W_{\Delta\lambda_2}$ is the energy radiated in the shorter-wavelength band $\Delta\lambda_2$ ($\Delta\lambda_2 = 0 - 2000 \text{ \AA}$) and absorbed by the walls of the discharge tube.

The energy Q was calculated from the current-voltage characteristics. Estimates of the values of E_{ev} and E_{kin} show that they can be neglected. U and I were calculated from the brightness temperature of the discharge and from the theoretical $z(T)$ dependence, while W was calculated as for absolute black-body radiation.

Let us consider a discharge made up by explosion of a silver wire of 0.1 mm diameter at $U_0 = 20 \text{ kV}$. Figure 9 shows the results of calculations of the electric energy Q (curve 1), the energy radiated in the quartz transparency band $W_{\Delta\lambda_1}$ (2), and also the values of U (triangle)

and I (square) at the instant of the current maximum. As to $W_{\Delta\lambda_2}$, calculation of this quantity by means of the formula for absolute black-body radiation leads to a value that exceeds the entire energy delivered to the discharge. This indicates that at its prevailing temperatures of 2 – 4 eV, the discharge is not opaque to the short-wave quanta. This "greyness" of the radiation can easily be accounted for by introducing a factor $\xi(x_0)$. The value of x_0 was obtained by solving Eq. (2.6), using the experimental value for r_d and for $l_\nu(x_0)$ the usual expression for the spectral free path in the case of multiple ionization in the Kramers-Unsold approximation:

$$l_\nu = 5 \cdot 10^{22} \frac{T^{3/2} x^3}{(1+x)^2 z N^2 (e^x - 1)},$$

in which we substituted the experimental value of the brightness temperature and the theoretical value of the average concentration of the charged particles. Calculation in accordance with this scheme leads to a value $W_{\Delta\lambda_2} \approx 1$ kJ for the instant of the current maximum. Thus, the energy balance in the discharge has the following characteristics at that instant of time: the energy input is $Q \approx 3$ kJ, and the dissipated energy is

$$U + I + W_{\Delta\lambda_1} + W_{\Delta\lambda_2} \approx 2.5 \text{ kJ}.$$

These data demonstrate the good agreement between the energy input and dissipation, if it is recognized that the losses at the electrodes are not taken into account in the balance. Thus, out of the 3 kJ delivered to the discharge, one-third is carried away by the radiation in the transparency band of the quartz and approximately one-third is carried away by radiation of shorter wavelengths and is absorbed by the discharge tube. We note that a qualitatively similar result was obtained also for discharge in lithium^[10].

Figure 9 also shows the results of photoelectric measurements of the energy radiated in the spectral intervals $\Delta\lambda_3 = 2300 - 3300 \text{ \AA}$ and $\Delta\lambda_4 = 3360 - 4300 \text{ \AA}$, from which it follows, in particular, that approximately half of the total outgoing radiation is radiated in the ultraviolet region.

We present now the principal data on long (40 and 96 cm) discharges investigated with the second setup. The experiments have shown that in this case there exists a rather large time interval during which the discharge radiates like an absolute black body and during which the main energy input to the discharge takes place. This interval is the first quasi-half-cycle of the discharge current. Indeed, for discharges 40 and 96 cm long at a voltage $U_0 = 15$ kV, the inputs during this time (75 and 85 μsec , respectively) are 38 and 36 kJ, amounting to $\sim 68\%$ and $\sim 64\%$ of the total energy stored in the capacitor bank. During this time, approximately 12.5 kJ is radiated in the transparency band of quartz, i.e., again one-third of the total energy input. Finally, measurements of the total radiation energy during the entire discharge show that the energy radiated in the transparency band of quartz is 20 kJ, i.e., about 35% of the entire energy stored in the setup.

7. CONCLUSION

Our analysis shows that the entire aggregate of the experimental data obtained in this study fits well within the framework of the theory of self-contracted discharges in an optically dense plasma. For the case of absorption of light by multiply ionized atoms, neither the equi-

Type of pump source	IFP-5000	"Soviet" flashlamp, UF900/20	Lithium discharge in vacuum (FIAN)	Explosion in air, 24 kV (MGU)	Explosion in vacuum, 15 kV	Explosion in vacuum, 17 kV
Discharge length (cm)	25	90	14,5	75	40	96
Length of principal phase of the discharge τ (μsec)	620	150	70	55	75	86
Capacitor-bank energy & (kV)	5	20	26,5	83	56	72
Total energy delivered to discharge Q (kJ)	4	16	17,5	60	38	51
Brightness temperature at maximum (10^4 K)	9000	11000	17000	26000	26000	24000
Total radiation energy W (kJ)	2.6	—	6.7	38	20	29
Energy radiated in the band $2200 < \lambda < 2700 \text{ \AA}$, $W_{\Delta\lambda_3}$ (kJ)	0.2	1.0	1.03	4.4	3.1	2.9
Conversion coefficient $\eta = W/Q$ & (%)	50	—	25	45	36	40
Conversion coefficient in the ultraviolet $\eta_{\Delta\lambda_3} = W_{\Delta\lambda_3}/Q$ & (%)	4	5	4	5	5.5	4

librium characteristics of the discharge nor the region of existence of the opaque stage of the discharge depended on the plasma material. The discharge temperature T increases with increasing discharge current and with decreasing total number of particles per unit length of the discharge. The lifetime of the discharge is determined by the development of the surface mode of necking instability, the development increment of which is determined by the speed of sound. Most suitable from the point of view of developing a radiation source is apparently a discharge in the vapors of the heaviest elements, the current in which is close to the lower limiting value ~ 100 kA, while the necessary value of the temperature is determined by the total number of particles in the discharge.

The radiation plays the decisive role in the energy balance of the discharge, which is a highly efficient source of radiation. The characteristics of the investigated opaque discharges as radiation sources are listed in the table. For comparison, the table also gives the characteristics of xenon lamps and of discharges in lithium and in air^[25]. It follows from the table that the characteristics of the discharges in heavy-element vapors are at least no worse than those in a lithium discharge.

¹A. F. Aleksandrov and A. A. Rukhadze, Usp. Fiz. Nauk 105, 783 (1971) [Sov. Phys.-Usp 14, 814 (1972)].

²V. B. Rozanov and A. A. Rukhadze, Review Paper at 9th Internat. Conf. on Phenomena in Ionized Gases, Bucharest, 1969; FIAN Preprint No. 132, 1969.

³A. F. Aleksandrov, A. A. Rukhadze, and S. A. Triger, Proc. 9th Internat. Conf. on Phenomena in Ionized Gases, Bucharest, 1969.

⁴V. B. Rozanov, A. A. Rukhadze, and S. A. Triger, Prikl. Mekh. Tekh. Fiz. No. 5, 18 (1968).

⁵A. A. Rukhadze and S. A. Triger, FIAN Preprint No. 26, 1969.

⁶A. A. Rukhadze and S. A. Triger, Prikl. Mekh. Tekh. Fiz. No. 3, 11 (1968); FIAN Preprint No. 168, 1968.

⁷A. F. Aleksandrov, E. P. Kaminskaya, and A. A. Rukhadze, Prikl. Mekh. Tekh. Fiz. No. 1, 33 (1971).

⁸A. F. Aleksandrov and S. A. Reshetnik, ibid. No. 2, (1973).

⁹P. P. Volosevich, V. Ya. Gol'din, et al., op. cit.^[3], p. 348.

¹⁰A. D. Klementov, G. V. Mikhaïlov, et al., ibid., p. 350; in: Voprosy fiziki nizektemperaturnoi plazmy (Prob-

- lems of Low Temperature Plasma Physics), Nauka i tekhnika, Minsk, 1970, p. 269.
- ¹¹A. D. Klementov, G. V. Mikhaïlov, et al., *Teplofiz. Vys. Temp.* 8, 738 (1970).
- ¹²A. D. Klementov, F. A. Nikolaev, and V. B. Rozanov, *Proc. 11th Internat. Conf. on Phenomena in Ionized Gases*, London, 1971, p. 293.
- ¹³A. A. Vekhov, F. A. Nikolaev, and V. B. Rozanov, *Preprint FIAN No. 79*, 1971.
- ¹⁴E. Oktay, *D. Back, J. Appl. Phys.*, 41, 1716 (1970).
- ¹⁵F. A. Nikolaev, V. B. Rozanov, and Yu. P. Sviridenko, *3rd All-Union Conf. on Low Temperature Plasma Physics; abstracts of papers, Moscow, 1971; FIAN Preprint No. 99*, 1971.
- ¹⁶F. A. Nikolaev, V. B. Rozanov, and Yu. P. Sviridenko, *Kratkie soobshcheniya po fizike (FIAN)*, No. 4, 2 (1971).
- ¹⁷J. Katzenstein, *J. Appl. Phys.* 33, 718 (1962).
- ¹⁸C. Aycoberry, A. Brin, E. Delobbeau, P. Veyrie *Proc. V-th Intern. Conf. Ionization Phenom. in Gases, München, 1961*, p. 1952.
- ¹⁹E. K. Chekalin and V. S. Shumanov, *Zh. Tekh. Fiz.* 39, 71 (1969) [*Sov. Phys.-Tech. Phys.* 14, 46 (1969)].
- ²⁰V. S. Shumanov, *Zh. Prikl. Spektrosk* 14, 209 (1971).
- ²¹L. Niemyer, *Zs. Naturforsch* 24A, 1707 (1969).
- ²²A. F. Aleksandrov, V. V. Zosimov, A. A. Rukhadze, V. I. Savoskin, and I. B. Timofeev, *FIAN Preprint No. 72*, 1971.
- ²³A. F. Aleksandrov, V. V. Zosimov, A. A. Rukhadze, and V. I. Savoskin, *Kratkie soobshcheniya po fizike (FIAN)*, No. 6, 58 (1970).
- ²⁴A. F. Aleksandrov, V. V. Zosimov and I. B. Timofeev, *ibid.* No. 2, 25 (1972).
- ²⁵A. F. Aleksandrov, V. V. Zosimov, S. P. Kurdyumov, Yu. P. Popov, A. A. Rukhadze, and I. B. Timofeev, *Zh. Eksp. Teor. Fiz.* 61, 1841 (1971) [*Sov. Phys.-JETP* 34, 979 (1972)].
- ²⁶A. F. Aleksandrov, V. V. Zosimov, A. A. Rukhadze, V. I. Savoskin, and I. B. Timofeev, *3rd All-Union Conf. on Low Temperature Plasma Physics, abstracts of papers, Moscow, 1971*, p. 176.

Translated by J. G. Adashko
171